Inhibition of the mTORC1 pathway alleviates adipose tissue fibrosis

Sa Gong [a,b,1], Chang Li [a,1], Qingyang Leng [a], Chongxiao Liu [a], Yi Zhu [a], Hongli Zhang [a,**], Xiaohua Li [a,*]

[a] *Department of Endocrinology, Seventh People's Hospital of Shanghai University of Traditional Chinese Medicine, Shanghai, 200137, China*
[b] *Shanghai Songjiang District Fangta Hospital of Traditional Chinese Medicine, Shanghai, 201600, China*

ARTICLE INFO

ABSTRACT

Background: Adipose fibrosis is a major factor of adipose dysfunction, which causes metabolic dysfunction during obesity, but its molecular mechanisms are poorly understood. This study investigated the role and potential mechanisms of mTORC1 in obesity-induced adipose fibrosis.
Methods: ob/ob mice were injected with rapamycin or the same volume of normal saline. The level of fibrosis in epididymal adipose tissue (EAT) was detected by observing aberrant deposition of extracellular matrix. Expression of fibrotic related genes was analysed using RNA-seq. 3T3-L1 preadipocytes were treated with cobalt chloride (CoCl$_2$) and TGF-β1 to induce preadipocyte fibrosis. The fibrosis-related gene expression and protein levels were determined by RT-PCR, WB, and immunofluorescence in two types of fibrotic preadipocytes with or without rapamycin.
Results: Compared with vehicle treatment, EAT fibrosis-related aberrant deposition of extracellular matrix proteins and fibrotic gene expression were reduced in ob/ob mice treated with rapamycin. Both CoCl$_2$-induced hypoxia and TGF-β1 successfully promoted adipocyte fibrosis, and the upregulated fibrosis-related genes expression was inhibited after the mTORC1 pathway was inhibited by rapamycin.
Conclusion: Inhibition of the mTORC1 pathway ameliorates adipose fibrosis by suppressing fibrosis-related genes in hypoxia- and TGF-β-induced fibrotic preadipocytes.

1. Introduction

Obesity is a chronic and progressive disease caused by excessive accumulation and abnormal distribution of adipose tissue, and weight gain and systemic energy metabolism disorder are the main manifestations. It is associated with cardiovascular, respiratory, nervous, and other multisystem diseases [1]. According to the World Health Organization, more than 650 million adults were obese in 2016 [2], and this number is expected to rise to 1 billion by 2030 [3]. Currently, safe and effective prevention and treatment strategies for obesity are limited, so it is crucial to further clarify the cellular and molecular mechanisms underlying the prevention and treatment

* Corresponding author. Department of Endocrinology, Seventh People's Hospital of Shanghai University of Traditional Chinese Medicine, Shanghai, 200137, China.
** Corresponding author. Department of Endocrinology, Seventh People's Hospital of Shanghai University of Traditional Chinese Medicine, Shanghai, 200137, China.
E-mail addresses: hongliting@sina.com (H. Zhang), wendylee_tcm@shutcm.edu.cn (X. Li).
[1] These authors contributed equally to this work.

of obesity.

Adipose tissue is a highly dynamic organ that undergoes constant remodelling to adapt to a constantly changing metabolic environment related to obesity. When nutrients are present in excess, adipocytes store excess lipids until they reach the diffusional limit of oxygen. Initially, the hypoxic microenvironment induces angiogenesis and transfers the flexibility of the extracellular matrix (ECM), promoting adipose tissue to healthily expand to reduce hypoxia. However, as this state continues, chronic low-degree inflammation, fibrosis, cellular senescence, and necrotic adipocyte death will occur due to persistent hypoxia, ultimately leading to unhealthy adipose tissue remodelling, which is a major contributor to the systemic metabolic disturbances that are characteristic of obesity [4,5]. Adipose fibrosis is an important feature of severe obesity and a key obstacle to reversing obesity. It has historically been a challenge to find therapeutic targets to treat or alleviate adipose fibrosis.

The mechanistic target of rapamycin (mTOR), a serine/threonine kinase, is a major regulatory node that responds to changes in levels of nutrients and growth signals [6]. It forms the catalytic core of at least two functionally distinct signalling complexes, mTOR complex 1 (mTORC1) and mTOR complex 2 (mTORC2). However, rapamycin allosterically inhibits mTORC1 but not mTORC2, and most studies have discussed the regulation of mTORC1 and its role in metabolism [7]. Several studies have found that it plays important roles in lipid synthesis, adipocyte development and differentiation, and adipocyte function. In the ongoing exploration of the function of mTORC1, studies have shown that mTORC1 plays an important role in various fibrotic diseases, such as cardiac fibrosis, liver fibrosis, renal fibrosis, and pulmonary fibrosis [8–11]. It has been found that the mTORC1 pathway is activated in the adipose tissue of obese mice [12], but the roles of mTORC1 in adipose fibrosis have not been clarified.

In this study, we hypothesized that suppression of the mTORC1 pathway alleviates adipose tissue fibrosis. We utilized rapamycin to inhibit mTORC1 expression in obese mice and found that rapamycin reversed the morphology of adipose fibrosis and fibrotic genes expression in vivo. Then, we used preadipocytes treated with profibrotic drugs to explore the mechanism by which mTORC1 reverses adipose fibrosis. We demonstrated that mTORC1 reverses the expression of genes related to adipose tissue fibrosis at the protein, mRNA, and immunofluorescence levels. This study elucidated the effect of the mTORC1 pathway on alleviating adipose tissue fibrosis, which may constitute a treatment option for obesity.

2. Materials and methods

2.1. Animal experiments

Ten-week-old male homozygous ob/ob mice were purchased from SLAC (Shanghai, China) and kept in the SLAC Laboratory Animal Center Animal house. The mouse living environment temperature was 22–24 °C, and the light/dark period was 12 h. The ob/ob mice were randomly divided into two groups after one week of adaptive feeding.

The ob/ob mice in the rapamycin group were intraperitoneally injected with rapamycin (0.5 mg/kg/day) for two weeks. The vehicle group was given the same volume of normal saline injection. After two weeks, the mice were killed, and epididymal adipose tissue (EAT) was taken. Body weight and fasting blood glucose were measured before and after injection.

Table 1
Primers used for quantitative real-time PCR.

Gene	Sequence
actin	F- TGTACCCAGGCATTGCTGAC
	R- CTGCTGGAAGGTGGACAGTG
Col1a1	F- TGCTGGTCCCAAAGGTTC
	R- CAGGGCGACCATCTTGAC
LOX	F- TCCGCAAAGAGTGAAGAACC
	R- CATCAAGCAGGTCATAGTGG
Loxl2	F- ATTAACCCCAACTATGAAGTGCC
	R- CTGTCTCCTCACTGAAGGCTC
α-SMA	F- TCCCAGACATCAGGGAGTAA
	R- TCGGATACTTCAGCGTCAGGA
TIMP-1	F- ATCTGGCATCCTCTTGTTG
	R- CGCTGGTATAAGGTGGTCTC
MMP3	F- TTAAAGACAGGCACTTTTGGCG
	R- CCCTCGTATAGCCCAGAACT
Smad2	F- CCAACTGTAACCAGAGATACGGC
	R-AACCCTGGTTGACAGACTGAGC
Smad3	F- GTCAAAGAACACCGATTCCA
	R-TCAAGCCACCAGAACAGAAG
TGF-β1	F- TGATACGCCTGAGTGGCTGTCT
	R-CACAAGAGCAGTGAGCGCTGAA
Smad4	F- CAGCCATAGTGAAGGACTGTTGC
	R- CCTACTTCCAGTCCAGGTGGTA

2.2. Cell culture and treatment

Mouse 3T3-L1 preadipocytes were purchased from the ATCC cell bank. The 3T3-L1 preadipocytes were plated in 24-well plates and incubated in 10 % foetal bovine serum-DMEM at 37 °C in a 5 % CO_2 atmosphere. Once 3T3-L1 preadipocytes reached 80 % confluence, they were used for subsequent experiments.

Preadipocytes were treated with different concentrations of cobalt chloride ($CoCl_2$) (Sigma, USA) (0 , 50, 100, 200, 400, 800 μmol/ l) for 12 h or 24 h to induce hypoxic conditions. Then, the preadipocytes were pretreated with $CoCl_2$ for 6 h and treated with or without rapamycin (Sigma, USA) (5, 10, 50 nmol/l) for 12 h and 24 h and collected for subsequent experiments.

Different concentrations of recombinant mouse transforming growth factor beta 1 (TGF-β1) (Cell Signalling Technology (CST), USA) (0, 5, 10, 50 ng/ml) were administered for approximately 24 h and 48 h for follow-up experimental studies. After inducing preadipocyte fibrosis, the preadipocytes were treated with or without different concentrations of rapamycin (5, 10, 50 nmol/l) for 24 h and 48 h and collected for follow-up experiments.

2.3. Real-time PCR analysis

Total RNA was isolated from cells or adipose tissues using an RNeasy Plus Mini Kit (Qiagen, Hilden, Germany). Complementary DNA (cDNA) was prepared using a PrimeScript™ RT Reagent Kit (Vazyme, Nanjing) according to the manufacturer's instructions. Real-time PCR was performed in a Light Cycler 480 II Real-Time PCR system (Roche Diagnostics, Basel, Switzerland) using SYBR® Green (Vazyme, Nanjing). The sequences of the primers are shown in Table 1. The mRNA level was quantitated by the $2^{-\Delta\Delta Ct}$ method and normalized to the level of actin mRNA.

2.4. Western blotting assay

The concentrations of proteins in cells or adipose tissue lysates were quantitated by BCA protein assay (Beyotime, Shanghai). Protein samples (20 μg) were separated by electrophoresis in an 8 % SDS−PAGE gel and transferred to a polyvinylidene fluoride membrane, followed by immunoblotting according to the protocol outlined by Cell Signalling Technology (CST). The blotted membrane was developed with ECL Advance (CST) and imaged with a LAS-4000 Super CCD Remote Control Science Imaging System (GE). The primary antibodies used were specific to the following proteins: tubulin (Sigma, USA), β-actin (CST, USA), GAPDH (CST, USA), phospho-S6 ribosomal protein (PS6) (Ser235/236) (CST, USA), hypoxia-inducible factor 1-alpha (HIF-1α) (CST, USA), alpha smooth muscle actin (α-SMA) (Abcam, UK), and tissue inhibitor of metal protease 1 (TIMP-1) [EPR16616] (Abcam, UK). The secondary antibodies used were HRP-conjugated goat anti-rabbit IgG (H + L) (BioTNT, China) and HRP-conjugated goat anti-mouse IgG (H + L) (Bio TNT, China).

2.5. RNA-seq analyses

A total amount of 1 μg qualified RNA per sample was used as input material for library preparation. Sequencing libraries were generated using ScriptSeq v2 (Illumina) following the manufacturer's recommendations. The library preparations were sequenced on an Illumina HiSeq X Ten. STAR (v2.5) was used to determine the number of coding genes in each sample.

2.6. Sirius Red staining and Masson's trichrome staining

The 6 μm sections of EAT were deparaffinized and rehydrated for Masson's trichrome staining and Sirius Red staining. For Masson's trichrome staining, the sections were stained with Weigert's iron haematoxylin and rinsed with distilled water. Then, the sections were incubated with Biebrich scarlet acid fuchsin solution and rinsed again three times with distilled water. The sections were treated with a phosphotungstic acid-phosphomolybdic acid solution and then directly stained with an aniline blue solution. The sections were treated with 1 % acetic acid solution and dehydrated with 95 % alcohol and anhydrous ethanol. After dehydration, the sections were cleaned and sealed. For Sirius Red staining, the sections were rinsed with distilled water and stained with Sirius scarlet - picric acid stain solution for 1 h. After dehydration and cleaning with xylene, the sections were mounted.

2.7. Immunofluorescence staining

For cell immunofluorescence staining, cells cultured on coverslips were washed with cold PBS twice and then fixed with cold methanol: acetone (1:1) for 15 min at 20 °C. Following 3 washes with PBS containing 0.5 % BSA, the cells were blocked with 0.1 % Triton X-100 and 2 % BSA in PBS buffer for 30 min at room temperature and then incubated with specific primary antibody (α-SMA [SP171] (Abcam, UK)) and secondary antibody (Goat anti-Rabbit IgG (H + L), Alexa Fluor™ 488 (Beyotime, China)) as described above. Cell nuclei were double-stained with DAPI.

2.8. Statistical analysis

Data are expressed as the means ± SEMs. GraphPad Prism 8.0.2 was used for recording and plotting. SPSS 20.0 software was used for statistical analysis. One-way ANOVA was used to compare the mean among the three groups. In pairwise comparisons between

groups, if the variance was homogenous, the LSD method was used for statistical analysis; otherwise, Dunnett's T3 test was used. $P < 0.05$ was considered statistically significant.

3. Results

3.1. Inhibition of mTORC1 alleviates adipose fibrosis in ob/ob mice

To investigate whether the mTORC1 pathway is involved in adipose fibrosis, male ob/ob mice aged 11 weeks were intraperitoneally injected with vehicle or the mTORC1 inhibitor rapamycin for 2 weeks. There were no differences in body weight or fasting blood glucose (FBG) between the two groups either before or after injection (Fig. 1A and B). The ribosomal protein S6 (S6) is the classical substrate and major effector of mTORC1 [13,14]. To further confirm that rapamycin indeed inhibited the mTORC1 pathway, we further examined the phosphorylation levels of S6 in epididymal adipose tissue (EAT), which is one of the most classical tissues for adipose fibrosis in mice [15]. Consistent with our expectations, the phosphorylation levels of S6 in the rapamycin group were significantly downregulated compared with those in the vehicle group (Fig. 1C). The results indicated that rapamycin successfully inhibited the mTORC1 signalling pathway but did not significantly change glucose level or body weight in obese mice, at least in the short term. To detect the deposition of collagen fibres, we performed Sirius red staining and Masson's trichrome staining on the EAT in mice. Compared to the vehicle group, the rapamycin group exhibited reduced collagen deposition in EAT sections (Fig. 1D and E). These studies indicate that inhibition of the mTORC1 pathway directly ameliorates adipose fibrosis.

3.2. Inhibition of mTORC1 reduces fibrotic gene expression

To further evaluate the effect of the mTORC1 pathway on adipose fibrosis, RNA-seq was carried out on EAT from rapamycin-treated and control mice. After processing the raw data, gene expression profiling data was obtained, including gene symbol, gene description, and read count of each gene. Initially, we performed principal component analysis (PCA) based on fibrosis-related genes to obtain an overall picture of adipose fibrosis regulated by mTORC1. In the PCA plot, fibrosis-related genes in the two groups were completely separated (Fig. 2A). Next, analysis of the differential expression of fibrotic genes between rapamycin-treated mice and control mice revealed reduced expression of some fibrosis marker genes in the rapamycin-treated group compared to the control group (Fig. 2B). To confirm the RNA-seq analysis, we analysed the mRNA expression of 9 selected genes, including ECM components (Col1a1, Col3a1, Col6a1, and Fn1), matrix metalloproteinases (Mmp2, Mmp3, Timp1), and cross-linking enzymes (Lox and Loxl2), by real-time quantitative RT–PCR. We detected significantly reduced expression of Cola1, Col3a1, Col6a2, Mmp3, Timp1, and Lox (Fig. 2C) in
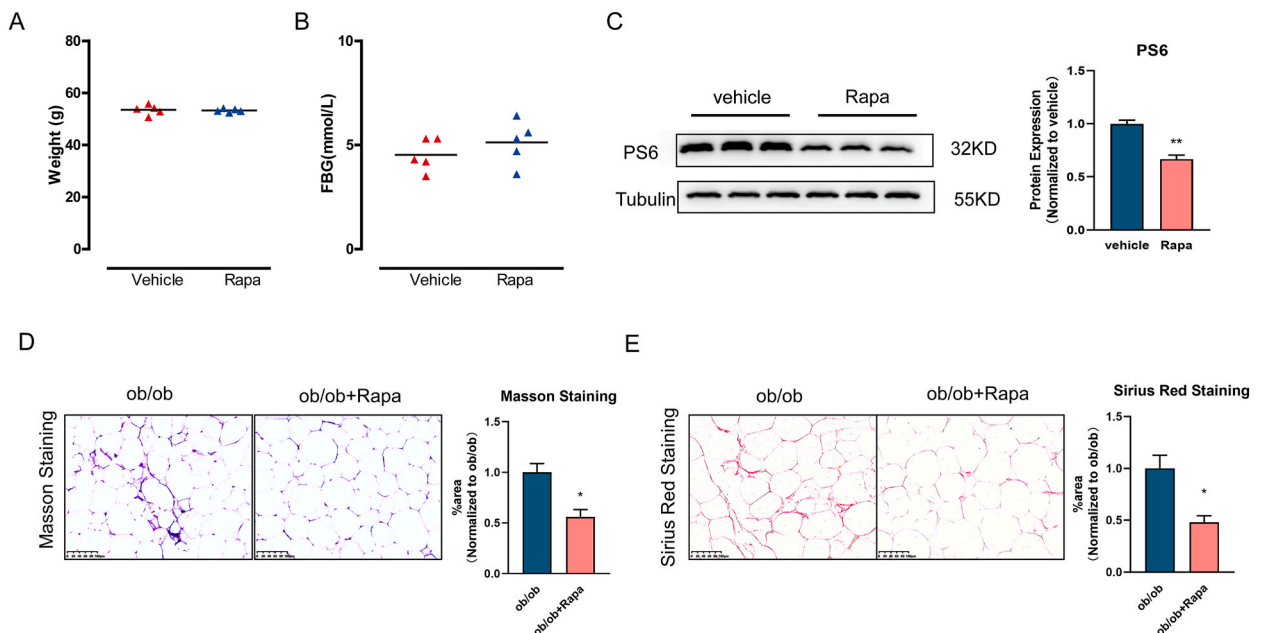

Figure 1. Inhibition of the mTORC1 pathway alleviates adipose fibrosis in ob/ob mice **A, B**: Body weight (g) (A) and fasting blood glucose (mmol/l) (B) of ob/ob mice treated with rapamycin (0, 0.5 mg/kg/days) for 14 days (n = 5 per group). **C**: Representative Western blots showing the protein levels of phosphorylated S6 in the EAT of ob/ob mice treated with rapamycin (0, 0.5 mg/kg/day) for 14 days. Densitometric analysis of band intensity relative to Tubulin and normalized to the group of vehicle. **D, E**: Representative images and quantification of Masson's trichrome (collagen appears blue) and Sirius Red staining (collagen appears red) of EAT of ob/ob mice treated with rapamycin (0, 0.5 mg/kg/day) for 14 days. The data are expressed as the mean ± SEM. *$P < 0.05$, *$P < 0.01$, *$P < 0.001$. P values (95 % CI) were determined by 2-tailed t-test.
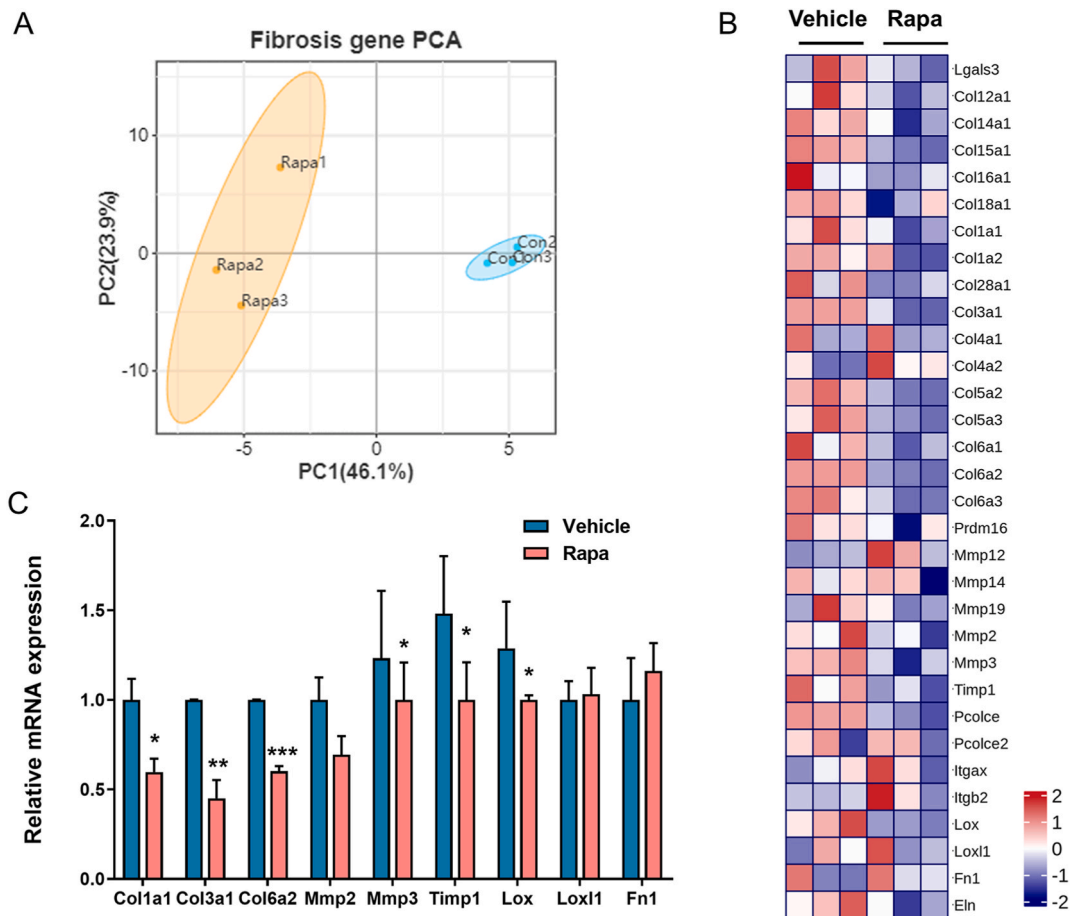
Figure 2. Inhibiting the mTORC1 pathway reduces fibrotic gene expression in EAT **A**: Two-dimensional PCA based on the fibrosis-related gene cluster between rapamycin-treated mice and control mice. **B**: Heatmap of the differentially expressed genes involved in adipose fibrosis in EAT of rapamycin-treated and control mice. **C**: RT−PCR analysis of fibrotic genes in EAT of rapamycin-treated and control mice. Data are presented as the mean ± SEM, *$P < 0.05$, *$P < 0.01$, *$P < 0.001$. P values (95 % CI) were determined by 2-tailed t-test.

rapamycin-treated mice, which coincides with the results of RNA-seq. Our data demonstrate that inhibition of the mTORC1 pathway decreased the expression of fibrotic genes.

3.3. Inhibition of mTORC1 reverses the adipose fibrosis induced by hypoxia

To further clarify the specific mechanism of mTORC1 in adipose fibrosis, we first explored the role of mTORC1 in hypoxia, which represents the early progression stage of adipose fibrosis [4,16]. In hypoxic adipose tissue, the increased expression of hypoxia-inducible factor 1-alpha (HIF-1α) enhances the synthesis of ECM components and stabilizes collagen [16]. To induce the preadipocytes to achieve this hypoxic condition for further study, we treated preadipocytes with different concentrations of cobalt chloride ($CoCl_2$) for 24 h. The results showed that $CoCl_2$ promoted the protein expression of HIF-1α in a dose-dependent manner, and the low dose of $CoCl_2$ (100 μM) had a significant effect on preadipocytes (Fig. 3A). Hypoxia-induced fibrosis causes mild upregulation of TGF-β1 expression within 24 h, but does not up-regulate downstream targets of TGF-β1, so fibrosis induced within 24 h is mainly related to hypoxia(Fig. 3B).Then, we analysed the mRNA expression of fibrotic genes, including Col1a1, Mmp3, Lox and Loxl2, in preadipocytes with or without $CoCl_2$ treatment (100 μM and 200 μM) for 12 or 24 h. The results showed that the mRNA levels of these fibrotic genes were significantly upregulated after treatment with $CoCl_2$ for 12 or 24 h in preadipocytes (Fig. 3C–F). Consistent with this, the immunofluorescence results in Fig. 3G show that the preadipocytes in the control group expressed a basal level of α-smooth muscle actin (α-SMA), a marker of myofibroblasts. $CoCl_2$ induced a significant increase in α-SMA expression, showing fibrogenic activation of the preadipocytes. Our data demonstrate that $CoCl_2$ can successfully induce hypoxia to initiate adipose fibrosis.

To determine whether mTORC1 participates in the activation of fibrotic genes, preadipocytes were pretreated with $CoCl_2$ (100 μM) for 6 h and then treated with increasing concentrations of rapamycin (24 h). Then, we detected the phosphorylation levels of S6 and found that rapamycin significantly downregulated the phosphorylation levels of S6 in fibrotic preadipocytes (Fig. 4A), suggesting that rapamycin successfully inhibited the activation of the mTORC1 pathway in the progression of adipose fibrosis. Furthermore, the
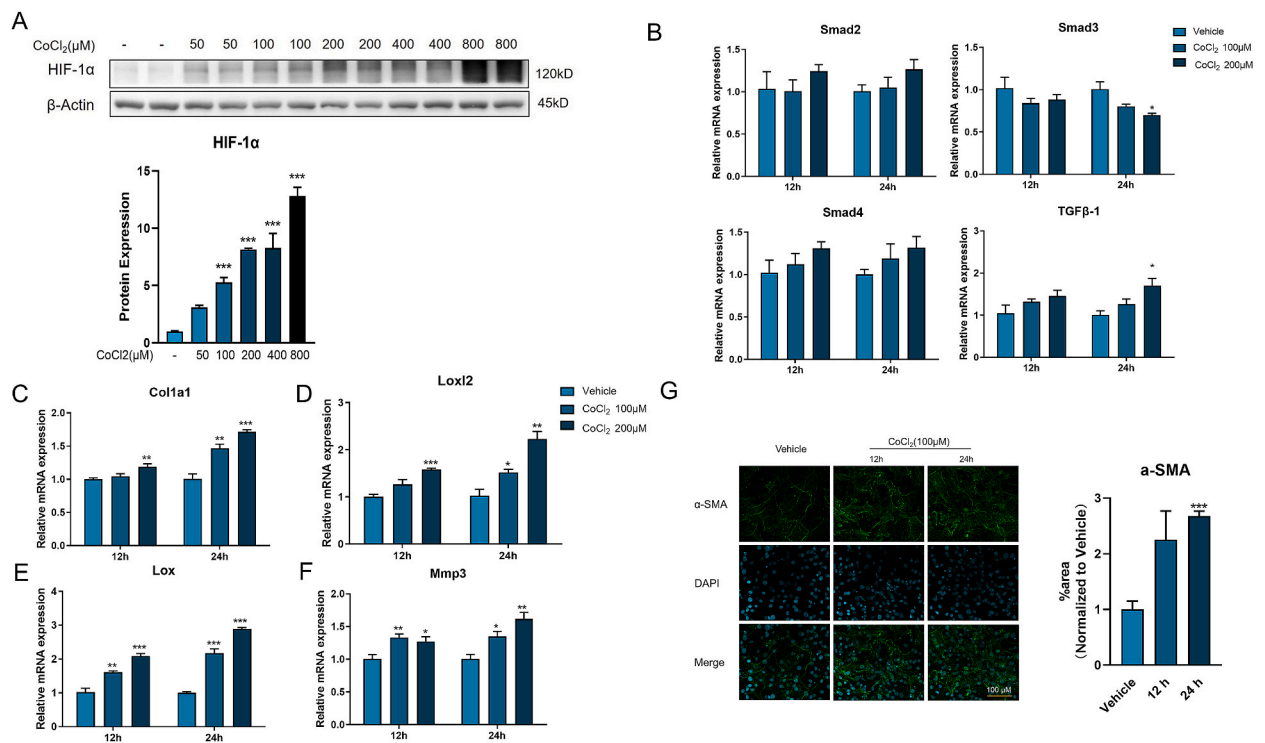
Figure 3. CoCl$_2$ induces hypoxia to initiate preadipocyte fibrosis **A**: Representative Western blots showing the protein levels of HIF-1α in preadipocytes treated with CoCl$_2$ (0, 50, 100, 200, 400, 800 μM) for 24 h. β-Actin was used as a loading control. Densitometric analysis of band intensity relative to β-actin and normalized to the group of CoCl$_2$ (0 μM). **B–F**: The mRNA expression of Smad2, Smad3, Smad4, TGF-β1, Col1a1, Loxl2, LOX, and Mmp3 in preadipocytes treated with CoCl$_2$ (0, 100, 200 μM) for 12 and 24 h (n = 4). G Preadipocytes were treated with CoCl$_2$ (0, 100 μM) for 12 h or 24 h. Preadipocytes were stained with α-SMA (green) and nuclei (DAPI, blue). Fibrosis activation was quantified as percentage of α-SMA stress fiber positive cells. Independent experiments were performed three times with similar results. The data are expressed as the mean ± SEM. *P < 0.05, *P < 0.01, *P < 0.001. P values (95 % CI) were determined by one-way ANOVA.

expression levels of genes related to hypoxia-induced adipocyte fibrosis were detected, and CoCl$_2$-induced protein expression of HIF-1α, mRNA expression of fibrotic genes, and the fluorescence level of α-SMA were inhibited by rapamycin (Fig. 4B–G). These data indicate that the inhibition of mTORC1 can reverse adipose fibrosis induced by hypoxia to a certain extent.

3.4. Inhibition of mTORC1 ameliorates adipose fibrosis induced by TGF-β1

Transforming growth factor beta 1 (TGF-β1) is the master regulator of fibrosis, which activates fibroblasts and myofibroblasts and accelerates ECM accumulation [17,18]. It is often used to induce fibrosis in various cells in vitro [19,20]. Therefore, to further confirm whether the inhibition of mTORC1 could reverse adipose fibrosis, we selected the TGF-β1-induced adipose fibrosis model. We treated preadipocytes with different concentrations of TGF-β1 for 24 and 48 h, and increased the mRNA level of Smad3 which is the classic downstream genes of TGF-β1(Fig. 5B). As we hypothesized, TGF-β1 significantly increased the protein levels of α-SMA and tissue inhibitors of metalloproteinases (TIMP1), the mRNA levels of fibrotic genes (Col1a1, LOX, Loxl2 and TIMP-1), and the fluorescence level of α-SMA in preadipocytes (Fig. 5A, C-G). This result suggested that TGF-β1 can successfully induce preadipocyte fibrosis in vitro. Then, we cotreated the preadipocytes with rapamycin and TGF-β1. Rapamycin successfully inhibited the phosphorylation of the S6 protein (Fig. 6A), suggesting that rapamycin inhibited the mTORC1 pathway. TGF-β1-induced increases in the Smad3 mRNA was no difference by cotreatment with rapamycin (Fig. 6B). TGF-β1-induced increases in the protein levels of α-SMA and TIMP1, the mRNA levels of fibrotic genes (Col1a1, LOX, Loxl2 and TIMP-1), and the fluorescence levels of α-SMA in preadipocytes were markedly reduced by cotreatment with rapamycin (Fig. 6C–H). These results indicate that mTORC1 is involved in the pathogenesis and development of adipose tissue fibrosis.

4. Discussion

Adipose fibrosis is a major factor of adipose dysfunction, which causes metabolic dysfunction during obesity. There is little research into targets and therapies for adipose fibrosis, which is historically a challenging research area and a popular research topic. In this study, we found that the mTORC1 pathway is an important target for improving adipose fibrosis. The in vivo experiments showed that the successful inhibition of the mTORC1 pathway could directly induce the morphological reversal of adipose fibrosis and reduce
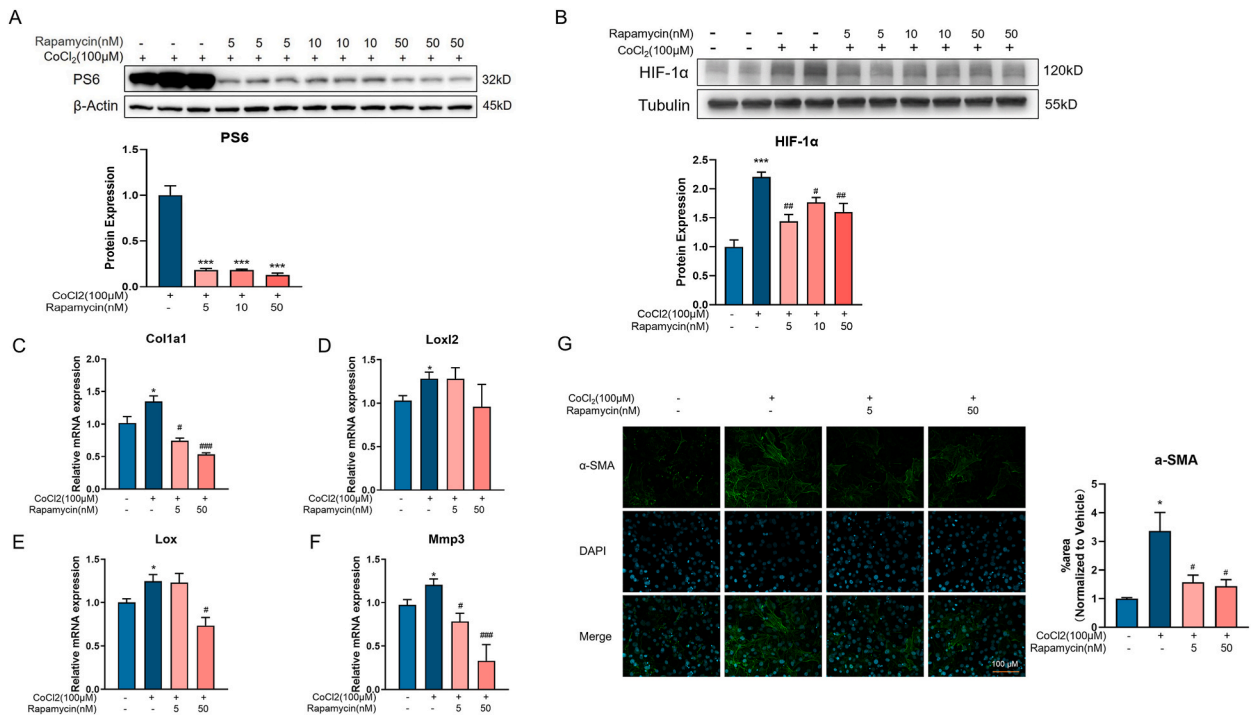
Figure 4. Inhibition of mTORC1 reverses the adipose fibrosis induced by hypoxia **A, B**: Representative Western blots showing phosphorylation of S6 and HIF-1α in preadipocytes treated with rapamycin (0, 5, 10, 50 nM) for 24 h in the absence or presence of CoCl$_2$ (100 μM). β-actin and Tubulin were used as loading controls. Densitometric analysis of band intensity relative PS6 and HIF-1α. **C–F**: The mRNA expression of Col1a1, Loxl2, LOX, and Mmp3 in preadipocytes treated with rapamycin (0, 5, 50 nM) for 12 h in the absence or presence of CoCl$_2$ (100 μM) (n = 4). **G**: Preadipocytes were treated with rapamycin (0, 5, 50 nM) for 24 h in the absence or presence of CoCl$_2$ (100 μM). Preadipocytes were stained with α-SMA (green) and nuclei (DAPI, blue). Fibrosis activation was quantified as percentage of α-SMA stress fiber positive cells. Independent experiments were performed three times with similar results. The data are expressed as the mean ± SEM. *$P < 0.05$, *$P < 0.01$, *$P < 0.001$. P values (95 % CI) by 2-tailed *t*-test relative to the samples without CoCl$_2$. #$P < 0.05$, ##$P < 0.01$, ###$P < 0.001$. P values (95 % CI) were determined by one-way ANOVA relative to control samples.

fibrotic gene expression in ob/ob mice. In vitro, we found that the expression of fibrosis-related genes in preadipocytes treated with CoCl$_2$ or TGF-β1 was markedly reduced by cotreatment with rapamycin. Our study provides a new research point and direction for further prevention and treatment of adipose fibrosis.

The underlying mechanism of adipose fibrosis is the excessive deposition of ECM components (mainly cross-linked collagens) and impaired degradation, which is caused by an adverse repair process involving hypoxic angiogenesis and an inflammatory cascade reaction, accompanied by tissue thickening and scarring that leads to irreversible adipose morphological and functional changes [4, 21]. To date, existing reports have mainly focused on tissues other than adipose. Despite increasing amounts of in-depth research on adipose fibrosis, the mechanisms have not been fully explained. The mTORC1 signalling pathway has long been reported to be a therapeutic target for a variety of tissue fibrotic diseases [10,11,22]. However, it was not until 2016 the mTORC1 pathway was found to be activated in the adipose tissue of obese mice [12]. The role of mTORC1 in adipose fibrosis remains unclear. We defined the role of mTORC1 in obesity-induced adipose fibrosis by intraperitoneally injecting rapamycin into ob/ob mice. Rapamycin successfully inhibited the mTORC1 pathway and ameliorated adipose fibrosis morphology changes. It is a truism that mTORC1, a major regulator of protein translation, regulates the mRNA transcription and translation of HIF-1α and other downstream genes through it's down-stream proteins (such as 1E-BP4, S1K6, STAT1, etc.). So, we examined tissue RNA-seq. The potential target of mTORC1 responsible for transcriptional regulation of the proteins involved in fibrosis was not clearly at present, but RNA-seq analysis further supported the phenotype results, and rapamycin decreased the expression of fibrotic genes, including ECM components, matrix metalloproteinases, and cross-linking enzymes. As we hypothesized, rapamycin, an mTORC1 inhibitor, functioned as it does in other fibrotic tissues [23, 24].

Adipose fibrosis can be induced by chronic hypoxia and inflammation during obesity, and it is significantly ameliorated after drastic weight loss [25,26]. In our study, the body weight of mice did not change after adipose fibrosis was improved, suggesting that inhibition of mTORC1 can directly reduce adipose fibrosis and has little relationship with body weight. In addition, adipose fibrosis can induce insulin resistance, and insulin resistance accelerates adipose fibrosis [21,27]. Studies have shown that the improvement of fibrosis can alleviate glucose metabolism by improving glucose uptake and insulin sensitivity in brown adipose tissue [28], while there is no evidence that insulin resistance can directly ameliorates adipose fibrosis. In our study, we found that glucose level did not change before or after inhibition of the mTORC1 pathway, at least in the short term. This suggests that the inhibition of mTORC1 by rapamycin
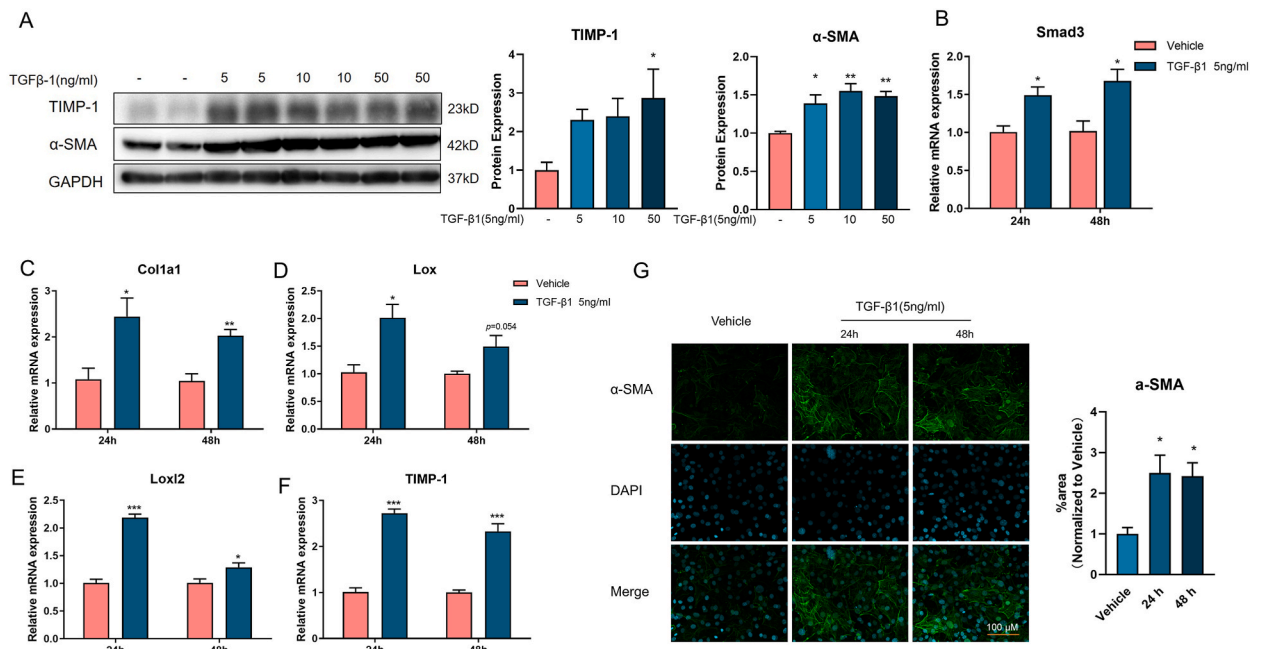
Figure 5. TGF-β1 induces preadipocyte fibrosis **A**: Representative Western blots and densitometric analysis of band intensity showing the protein levels of TIMP-1 and α-SMA in preadipocytes treated with TGF-β1 (0, 5, 10, 50 ng/ml) for 24 h. GAPDH was used as a loading control. **B–F**: The mRNA expression of Smad3, Col1a1, Loxl2, LOX, and TIMP-1 in preadipocytes treated with TGF-β1 (5 ng/ml) for 24 and 48 h (n = 4). **F**: Pre-adipocytes were treated with TGF-β1 (0.5 ng/ml) for 24 h or 48 h. Preadipocytes were stained with α-SMA (green) and nuclei (DAPI, blue). Fibrosis activation was quantified as percentage of α-SMA stress fiber positive cells. Independent experiments were performed three times with similar results. The data are expressed as the mean ± SEM. *$P < 0.05$, *$P < 0.01$, *$P < 0.001$. P values (95 % CI) by 2-tailed *t*-test relative to the vehicle.

improving adipose fibrosis is independent of whether insulin resistance is improved or not, and the improvement of adipose fibrosis has no benefit on glucose level in the short term.

Many factors can induce fibrosis, including obesity [29], ageing [30] and others. In this study, we mainly clarified the role of mTORC1 in adipose fibrosis caused by obesity. In the future, we will explore the roles of mTORC1 in adipose fibrosis caused by ageing and other factors that are still unclear. In addition, the ectopic adipose deposition caused by obesity causes fibrosis of the liver, kidney [31,32], and other organs. In this study, we mainly discuss the role of mTORC1 in the fibrosis of adipose tissue itself. In future investigations, we will further explore whether mTORC1 also plays roles in fibrosis of other tissues caused by ectopic adipose deposition.

After confirming that mTORC1 is indeed an important factor in the improvement of adipose fibrosis, we explored the specific role of mTORC1 in improving adipose fibrosis in vitro. Adipose fibrosis is a progressive process, and chronic hypoxia and chronic inflammation lead to fibrosis and scarring in adipose tissue. Chronic hypoxia increases the expression of HIF-1α, which can upregulate the expression of α-SMA and fibrotic genes, including ECM components, matrix metalloproteinases, and cross-linking enzymes, to induce adipose fibrosis [33–35]. Chronic inflammation promotes macrophage-secreted TGF-β, the master regulator of fibrosis, to activate fibroblasts and myofibroblasts and accelerate ECM accumulation [17]. CoCl$_2$ can induce cell hypoxia by upregulating HIF-1α [36], and TGF-β1 can induce fibrosis by upregulating mTORC1 [37]. Consistent with the above reports, we treated preadipocytes with CoCl$_2$ and TGF-β1 and found that CoCl$_2$ indeed increased the expression of HIF-1α, α-SMA and fibrotic genes. TGF-β1 increased the expression of TIMP-1, α-SMA and fibrotic genes. Therefore, the specific mechanism of mTORC1 was further studied based on exposing preadipocytes to similar hypoxic or inflammatory conditions by CoCl$_2$ or TGF-β1. In hypoxia-induced fibrotic preadipocytes, rapamycin successfully inhibited the mTORC1 pathway and downregulated HIF-1α expression and HIF-1α-induced fibrosis gene expression. In TGF-β1-induced fibrotic preadipocytes, rapamycin successfully inhibited the mTORC1 pathway and fibrosis gene expression. HIF-1α can induce an inflammatory environment to promote macrophages to secrete TGF-β1 [25,38], which can activate the PI3K/AKT/mTORC1 pathway [37], Smad3/α-SMA pathway [39] or other pathways to induce adipose fibrosis. This process is dependent on the assistance of macrophages. In our in vitro experiments, CoCl$_2$ was used to create a hypoxic state during the study. The fibrosis of preadipocytes, without coculture with macrophages or additional TGF-β1 treatment, was reversed by rapamycin. This suggests that the mechanisms by which rapamycin benefits the two types of fibrotic preadipocytes are different under different conditions. This needs to be studied further.

In conclusion, mTORC1 directly ameliorates obesity-induced adipose fibrosis and plays an important role in the development of obesity-induced fibrosis. We have discovered a new target for the prevention and treatment of adipose tissue fibrosis. In the future, we will continue to investigate the effect of mTORC1 inhibition in the two types of fibrotic preadipocytes. We will research the mechanism of mTORC1 in the fibrosis of other tissues caused by obesity or in adipose fibrosis caused by ageing and other factors.
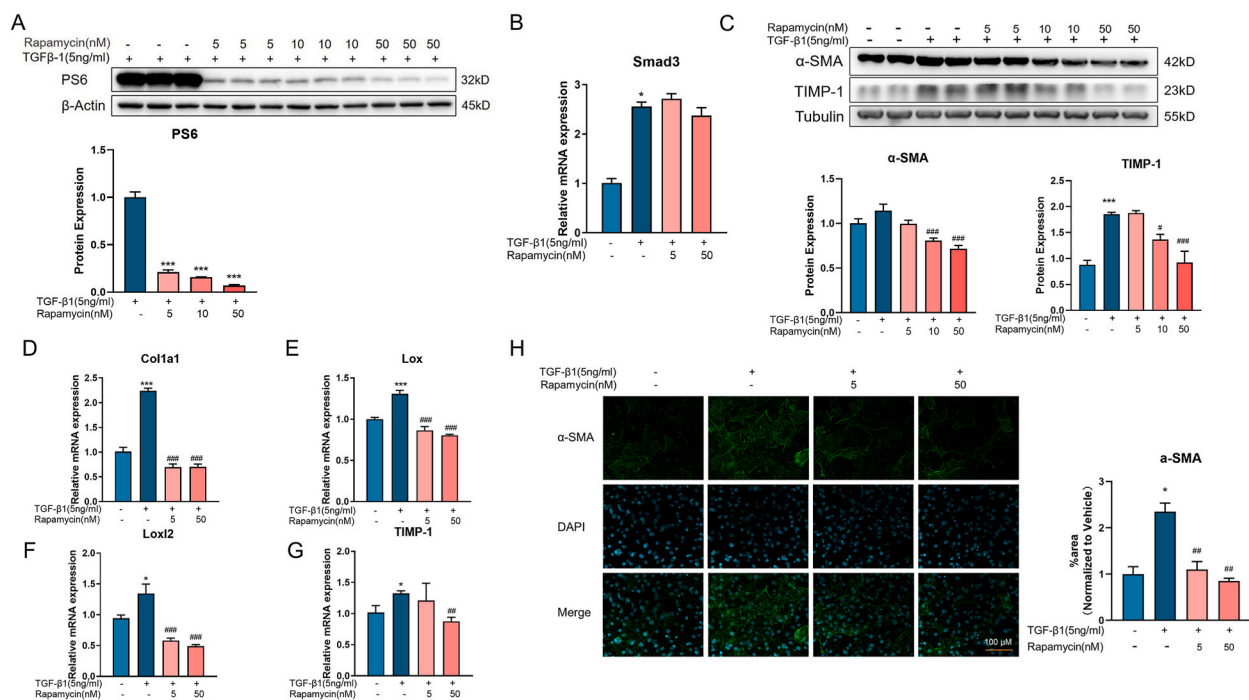
Figure 6. Inhibition of mTORC1 improves adipose fibrosis induced by TGF-β1 **A, C**: Representative Western blots and densitometric analysis of band intensity showing phosphorylation of S6 and HIF-1α in preadipocytes treated with rapamycin (0, 5, 10, 50 nM) for 24 h in the absence or presence of TGF-β1 (5 ng/ml). β-actin and Tubulin were used as loading controls. **B, D-F**: The mRNA expression of Smad3, Col1a1, Loxl2, LOX, and Mmp3 in preadipocytes treated with rapamycin (0, 5, 50 nM) for 24 h in the absence or presence of TGF-β1 (5 ng/ml) (n = 4). **G**: Preadipocytes were treated with rapamycin (0, 5, 50 nM) for 24 h in the absence or presence of TGF-β1 (5 ng/ml). Preadipocytes were stained with α-SMA (green) and nuclei (DAPI, blue). Fibrosis activation was quantified as percentage of α-SMA stress fiber positive cells. Independent experiments were performed three times with similar results. The data are expressed as the mean ± SEM. *$P < 0.05$, *$P < 0.01$, *$P < 0.001$. P values (95 % CI) by 2-tailed t-test relative to the samples without $CoCl_2$. #$P < 0.05$, ##$P < 0.01$, ###$P < 0.001$. P values (95 % CI) were determined by one-way ANOVA relative to control samples.

consent for publication

All authors approved the final version of the manuscript for publication.

Funding statement

Ethics statement

All procedures were according to the Institutional Animal Care and Use Committee of Shanghai SLAC Laboratory Animal Center (Ethics approval number: 20210425001).

Data availability statement

Data will be made available on Mendeley Data by https://doi.org/10.17632/nwt9frbd7h.1.

CRediT authorship contribution statement

Sa Gong: Writing – review & editing, Writing – original draft, Software, Methodology, Formal analysis. **Chang Li:** Writing – review & editing, Writing – original draft, Validation, Software, Methodology, Formal analysis, Data curation. **Qingyang Leng:** Software, Formal analysis, Data curation. **Chongxiao Liu:** Software, Formal analysis, Data curation. **Yi Zhu:** Software, Formal analysis, Data

curation. **Hongli Zhang:** Writing – review & editing, Writing – original draft, Supervision, Methodology, Investigation. **Xiaohua Li:** Writing – review & editing, Writing – original draft, Supervision, Project administration, Methodology, Investigation.

Declaration of competing interest

The authors declare that they have no known competing financial interests or personal relationships that could have appeared to influence the work reported in this paper.

Appendix A. Supplementary data

Supplementary data to this article can be found online at https://doi.org/10.1016/j.heliyon.2023.e21526.

References

[1] M. Kivimäki, T. Strandberg, J. Pentti, Solja T. Nyberg, Body-mass index and risk of obesity-related complex multimorbidity: an observational multicohort study, Lancet Diabetes Endocrinol. 10 (2022) 253–263.
[2] WHO, Obesity and Overweight, 2014. https://www.who.int/news-room/fact-sheets/detail/obesity-and-overweight, 2018.
[3] The World Obesity Federation, World Obesity Atlas 2022, 2022. https://www.worldobesity.org/resources/resource-library/world-obesity-atlas-2022, 2022.
[4] C. Crewe, Y.A. An, P.E. Scherer, The ominous triad of adipose tissue dysfunction: inflammation, fibrosis, and impaired angiogenesis, J. Clin. Invest. 127 (2017) 74–82.
[5] N. Ouchi, J.L. Parker, J.J. Lugus, K. Walsh, Adipokines in inflammation and metabolic disease, Nat. Rev. Immunol. 11 (2011) 85–97.
[6] A. Szwed, E. Kim, E. Jacinto, Regulation and metabolic functions of mTORC1 and mTORC2, Physiol. Rev. 101 (2021) 1371–1426.
[7] K. Huang, D.C. Fingar, Growing knowledge of the mTOR signaling network, Semin. Cell Dev. Biol. 36 (2014) 79–90.
[8] P. Polak, N. Cybulski, J.N. Feige, J. Auwerx, Adipose-specific knockout of raptor results in lean mice with enhanced mitochondrial respiration, Cell Metab 8 (2008) 399–410.
[9] H. Lian, Y. Ma, J. Feng, W. Dong, Heparin-binding EGF-like growth factor induces heart interstitial fibrosis via an Akt/mTor/p70s6k pathway, PLoS One 7 (2012), e44946.
[10] E. Patsenker, V. Schneider, M. Ledermann, H. Saegesser, Potent antifibrotic activity of mTOR inhibitors sirolimus and everolimus but not of cyclosporine A and tacrolimus in experimental liver fibrosis, J. Hepatol. 55 (2011) 388–398.
[11] E.K. Geissler, H.J. Schlitt, The potential benefits of rapamycin on renal function, tolerance, fibrosis, and malignancy following transplantation, Kidney Int. 78 (2010) 1075–1079.
[12] J. Han, H. Liang, D. Tian, J. Du, mTOR remains unchanged in diet-resistant (DR) rats despite impaired LKB1/AMPK cascade in adipose tissue, Biochem Bioph Res Co 476 (2016) 333–339.
[13] X. Wu, W. Xie, W. Xie, W. Wei, Beyond controlling cell size: functional analyses of S6K in tumorigenesis, Cell Death Dis. 13 (2022) 646.
[14] X.M. Ma, J. Blenis, Molecular mechanisms of mTOR-mediated translational control, Nat. Rev. Mol. Cell Biol. 10 (2009) 307–318.
[15] T. Khan, E.S. Muise, P. Iyengar, Z.V. Wang, Metabolic dysregulation and adipose tissue fibrosis: role of collagen VI, Mol. Cell Biol. 29 (2009) 1575–1591.
[16] E.C. Mariman, P. Wang, Adipocyte extracellular matrix composition, dynamics and role in obesity, Cell. Mol. Life Sci. 67 (2010) 1277–1292.
[17] X.M. Meng, D.J. Nikolic-Paterson, H.Y. Lan, TGF-beta: the master regulator of fibrosis, Nat. Rev. Nephrol. 12 (2016) 325–338.
[18] H. Shen, X. Huang, Y. Zhao, D. Wu, The Hippo pathway links adipocyte plasticity to adipose tissue fibrosis, Nat. Commun. 13 (2022) 6030.
[19] T. Guo, Z.L. Liu, Q. Zhao, Z.M. Zhao, A combination of astragaloside I, levistilide A and calycosin exerts anti-liver fibrosis effects in vitro and in vivo, Acta Pharmacol. Sin. 39 (2018) 1483–1492.
[20] N. Liu, L. Li, X. Zhu, Z. Ling, A high content screening assay to identify compounds with anti-epithelial-mesenchymal transition effects from the Chinese herbal medicine tong-mai-yang-xin-wan, Molecules (2016) 21.
[21] Megan K. DeBari, Rosalyn D. Abbott, Adipose tissue fibrosis: mechanisms, models, and importance, Int. J. Mol. Sci. 21 (2020).
[22] A. Yoshizaki, K. Yanaba, A. Yoshizaki, Y. Iwata, Treatment with rapamycin prevents fibrosis in tight-skin and bleomycin-induced mouse models of systemic sclerosis, Arthritis Rheumatol. 62 (2010) 2476–2487.
[23] M.J. Wu, M.C. Wen, Y.T. Chiu, Y.Y. Chiou, Rapamycin attenuates unilateral ureteral obstruction-induced renal fibrosis, Kidney Int. 69 (2006) 2029–2036.
[24] W. Wang, J. Yan, H. Wang, M. Shi, Rapamycin ameliorates inflammation and fibrosis in the early phase of cirrhotic portal hypertension in rats through inhibition of mTORC1 but not mTORC2, PLoS One 9 (2014), e83908.
[25] C. Henegar, J. Tordjman, V. Achard, D. Lacasa, Adipose tissue transcriptomic signature highlights the pathological relevance of extracellular matrix in human obesity, Genome Biol. 9 (2008) R14.
[26] Y. Liu, J. Aron-Wisnewsky, G. Marcelin, L. Genser, Accumulation and changes in composition of collagens in subcutaneous adipose tissue after bariatric surgery, J. Clin. Endocrinol. Metab. 101 (2016) 293–304.
[27] H.M. Lawler, C.M. Underkofler, P.A. Kern, C. Erickson, Adipose tissue hypoxia, inflammation, and fibrosis in obese insulin-sensitive and obese insulin-resistant subjects, J. Clin. Endocrinol. Metab. 101 (2016) 1422–1428.
[28] Y. Hasegawa, K. Ikeda, Y. Chen, D.L. Alba, Repression of adipose tissue fibrosis through a PRDM16-gtf2ird1 complex improves systemic glucose homeostasis, Cell Metab 27 (2018) 180–194.
[29] G. Marcelin, E.L. Gautier, K. Clement, Adipose tissue fibrosis in obesity: etiology and challenges, Annu. Rev. Physiol. 84 (2022) 135–155.
[30] Y. Li, N.T. Adeniji, W. Fan, K. Kunimoto, Non-alcoholic fatty liver disease and liver fibrosis during aging, Aging Dis 13 (2022) 1239–1251.
[31] R.F. Schwabe, I. Tabas, U.B. Pajvani, Mechanisms of fibrosis development in nonalcoholic steatohepatitis, Gastroenterology 158 (2020) 1913–1928.
[32] Justo Sandino, Marina Martín-Taboada, Gema Medina-Gómez, Rocío Vila-Bedmar, Novel insights in the physiopathology and management of obesity-related kidney disease, Nutrients 14 (2022).
[33] N. Halberg, T. Khan, M.E. Trujillo, I. Wernstedt-Asterholm, Hypoxia-inducible factor 1alpha induces fibrosis and insulin resistance in white adipose tissue, Mol. Cell Biol. 29 (2009) 4467–4483.
[34] Z. Michailidou, S. Turban, E. Miller, X. Zou, Increased angiogenesis protects against adipose hypoxia and fibrosis in metabolic disease-resistant 11β-hydroxysteroid dehydrogenase type 1 (HSD1)-deficient mice, J. Biol. Chem. 287 (2012) 4188–4197.
[35] R. Cancello, C. Henegar, N. Viguerie, S. Taleb, Reduction of macrophage infiltration and chemoattractant gene expression changes in white adipose tissue of morbidly obese subjects after surgery-induced weight loss, Diabetes 54 (2005) 2277–2286.
[36] N.K. Rana, P. Singh, B. Koch, CoCl(2) simulated hypoxia induce cell proliferation and alter the expression pattern of hypoxia associated genes involved in angiogenesis and apoptosis, Biol. Res. 52 (2019) 12.

[37] F. Das, N. Ghosh-Choudhury, L. Mahimainathan, B. Venkatesan, Raptor-rictor axis in TGFbeta-induced protein synthesis, Cell. Signal. 20 (2008) 409–423.

[38] Y.S. Lee, J.W. Kim, O. Osborne, D.Y. Oh, Increased adipocyte O2 consumption triggers HIF-1alpha, causing inflammation and insulin resistance in obesity, Cell 157 (2014) 1339–1352.

[39] Z. Michailidou, S. Turban, E. Miller, X. Zou, Increased angiogenesis protects against adipose hypoxia and fibrosis in metabolic disease-resistant 11beta-hydroxysteroid dehydrogenase type 1 (HSD1)-deficient mice, J. Biol. Chem. 287 (2012) 4188–4197.